Concrete-Plated Wooden Shear Walls: Structural Details, Testing, and Seismic Characterization

Luca Pozza, Ph.D.[1]; Roberto Scotta[2]; Davide Trutalli[3]; Andrea Polastri[4]; and Ario Ceccotti[5]

Abstract: This paper discusses the structural characterization of a novel hybrid shear-wall system formed by coupling standard platform-frame panels with an external reinforced concrete shelter formed of precast slabs screwed to the wooden frames. The external RC skin is intended as a supplementary bracing system, increasing strength and dissipative capacity of the bare timber frame. The structural performance of such hybrid shear wall under monotonic and cyclic loading was first theorized analytically on the basis of code provisions and then confirmed via experimental tests. The novel shear walls demonstrated to fulfill the requirements prescribed by Eurocode 8. In particular, the analyzed system belongs to high ductility class (HDC). Finally the seismic response of a reference building realized with the innovative hybrid shear walls was simulated by means of a numerical model validated on experimental tests; the suitable behavior factor for the building was estimated. **DOI: 10.1061/(ASCE)ST.1943-541X.0001289.** © *2015 American Society of Civil Engineers.*

Author keywords: Timber construction; Earthquake engineering; Seismic design; Ductility; Precast concrete; Wood structures.

Introduction

Structural skins are used in building practice to improve and adjust the robustness of buildings or to increase their thermohygrometric performances.

In Northern Europe and especially in United Kingdom, brick-clad timber frames have long been used, but the outer casing has only aesthetic and protective functions, with no structural function. This solution is not suitable for constructions in seismic areas because the external brick-clad area increases the overall mass of the building without improving its lateral shear resistance. In addition, the flexibility and ductility of the two structures (i.e., the internal wooden one and the brick cladding) differ and may interact with unpredictable effects during seismic events. In order to verify the true response of this kind of structural skin and specifications for the connection system between the external brick casing and the inner wooden shear walls, a six-story, TF2000, timber-frame building was tested at BRE Cardington in 2000 (Vahik 2006), in a project involving collaboration among public administrations, BRE, Trada Technology, and the timber industry.

In Canada and North America, mixed shear walls made of wood frames coupled with gypsum boards to improve lateral shear resistance have been extensively studied and are widespread (e.g., Karacabeyli and Ceccotti 1997). In the Alpine area and Northern Europe, construction systems composed of wooden frames braced by fiber-reinforced gypsum panels are becoming more common, and much research is ongoing to verify the structural response of this type of wall when subjected to horizontal force (e.g., Amadio et al. 2007).

This paper reports the results from an experimental, analytical, and numerical investigation about the seismic performance of a novel mixed structural system, which consists of a timber frame coupled with an external RC skin.

Description of the Construction System

The newly developed hybrid construction system combines a typical platform-frame shear wall with external RC slabs that act as a supplementary bracing system against horizontal forces. They also allow the creation of a ventilation chamber between the RC slabs and the wooden structure [Fig. 1(a)] that is open at the foundation and at the roof and continuous along the full height of the building. This chamber allows a continuous natural airflow behind the surface skin of the walls. Analytical and experimental evaluations of the thermal, hygrometric, and acoustic effectiveness of the ventilation chamber are still ongoing. Results will be published in a forthcoming work being such issues out of the scope of this work.

The proposed construction system is a modular one, in which mixed wood reinforced-concrete shear walls are made by connecting single precast modules having an aspect ratio of 3:1. Fig. 1(b) shows the basic modular panel as 3.24 m high and 1.08 m wide. It includes three RC slabs 108 × 108 × 4 cm. This size of RC slab was chosen for manufacturing restraints and considering the usual interstory height to be assured in residential buildings. The timber frame differs from that of standard platform-frame buildings since the spacing of vertical studs does not depend on OSB sheet size, but on that of the external concrete slabs.

The dimension of the concrete slabs influences the mechanical characteristics of the walls, but does not affect the idea of coupling RC slab with a timber platform frame. In this work only the 108 × 108-cm concrete slabs have been considered. Nevertheless the

[1]Civil Engineer, Dept. of Civil, Environmental and Architectural Engineering, Univ. of Padova, via Marzolo 9, 35131 Padova, Italy (corresponding author). E-mail: luca.pozza@dicea.unipd.it

[2]Research Associate and Civil Engineer, Dept. of Civil, Environmental and Architectural Engineering, Univ. of Padova, via Marzolo 9, 35131 Padova, Italy.

[3]Ph.D. Fellow and Civil Engineer, Dept. of Civil, Environmental and Architectural Engineering, Univ. of Padova, via Marzolo 9, 35131 Padova, Italy.

[4]Research Associate and Civil Engineer, Trees and Timber Institute of the National Research Council of Italy (CNR IVALSA), Via Biasi 75, 38010 San Michele all'Adige (TN).

[5]Associate Professor and Civil Engineer, IUAV, Univ. of Venezia, Italy.

Note. This manuscript was submitted on May 29, 2014; approved on January 26, 2015; published online on April 6, 2015. Discussion period open until September 6, 2015; separate discussions must be submitted for individual papers. This paper is part of the ***Journal of Structural Engineering***, © ASCE, ISSN 0733-9445/E4015003(12)/$25.00.

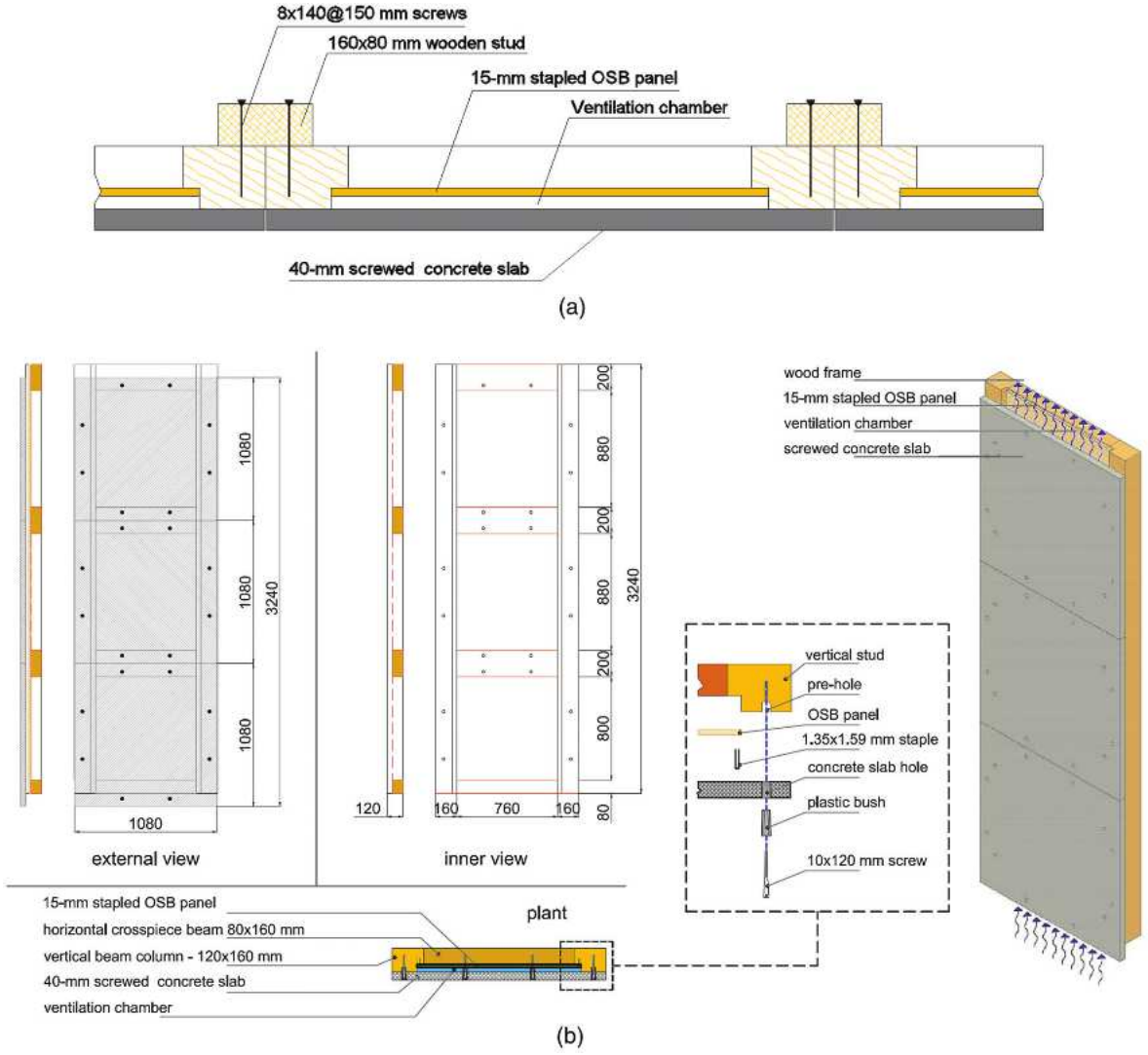

Fig. 1. (Color) View of preassembled modular panel: (a) detail of the ventilation chamber; (b) details of the system

analytical and experimental approaches hereafter given have a general validity.

The two structural systems forming the hybrid wood-concrete wall have different functions: gravity load is supported only by the wood-frame structure, which transfers its own weight and applied dead and live vertical loads to the foundations, whereas horizontal actions (i.e., wind and seismic shocks) are supported by both OSB sheets and RC slabs.

In the examined walls 15-mm thick OSB/3 panels are connected with 1.46×60-mm staples to the frame, while the RC slabs are connected to the frame with two 10×120-mm screws each side. Such screws are coupled with plastic bushes suitably designed to respond to particular functions—they reduce the clearance between the concrete slab and the screws without the need for sealants and they act as spacers between the horizontal cross beam of the wood frame and the concrete slab, creating the ventilation chambers.

Figs. 1 and 2 show details of the assembly of the modular panels and the fastening system of the RC slabs and Table 1 lists the detailed dimensions of the connections.

The slabs are reinforced with knitted steel wire mesh, $4@60 \times 60$ mm. Fig. 3 gives a detail of the RC slab.

Two adjacent modular panels are joined by a vertical wooden stud (rectangular section 160×80 mm) screwed to both panels

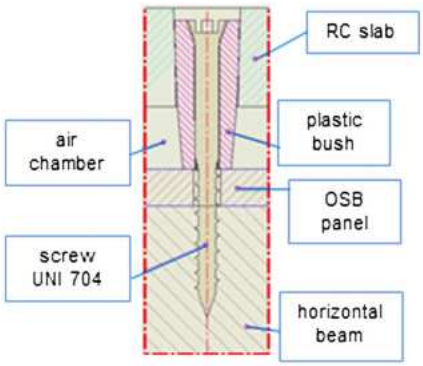

Fig. 2. (Color) Detail of plastic bush and screw

with $8 \times 140@150$ mm screws. This element also supports the floor and roof beams.

The modular wall panels are anchored to the foundations with hold-downs and bolts to avoid rocking and slip effects, respectively. The hold-downs are made of 3-mm press-belted L-profiles, made

Table 1. Detailed Dimensions of Connections and Anchoring

Connected components of a modular panel	Connectors		
	Type	Dimensions	Number/spacing
OSB panel to timber frame	Staples	$1.46 \times 12 \times 60$ mm	40 mm along the edge
RC slab to timber frame	Screws with plastic bush	10×120 mm	2 per side
Panel-to-panel connection with wooden stud (160×80 mm)	Screws	8×140 mm	150 mm
Timber frame to foundation	Hold-down	4×60 mm ring nails	$24 + 24$ per hold-down
	Bolts	12×80 mm	3

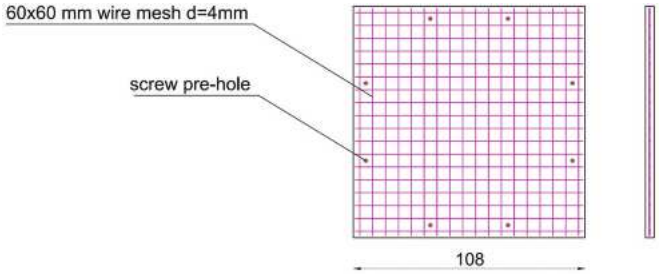

Fig. 3. (Color) Detail of the RC slab

with S275 galvanized steel, positioned in the corner between the vertical columns of a module and the joint cover stud. The hold-downs are nailed with twenty-four 4×60-mm ring nails per side to the vertical structure and connected to the concrete foundations with proper anchors, as standard hold-downs. In each panel both the bottom cross beam of the timber frame and the bottom concrete slab are fixed to the concrete foundation with 12-mm diameter concrete screws to prevent slip (Fig. 4). A more extensive description of the connection system and of the structural details specifically developed for this innovative building system can be found in Pozza (2013).

Analytical Evaluation of the Shear Resistance

Preliminary experimental tests were conduced to analyze separately the contribution to lateral resistance of the OSB panels and the RC slabs (Pozza 2013). Results showed that the two bracing systems reach the maximum resistance at almost the same ultimate displacement. This evidence defines the ultimate shear strength of each wall panel as the summation of the contributions of the two bracing systems. In any case it is limited by hold-downs and shear bolts capacities—the strength of the single panel is given by the weakest mechanism. In this section the strength of each mechanism is defined according to the analytical equations given in Eurocode 5 (CEN 2009).

The evaluation of the OSB-panel shear resistance is based on the provisions for staples according to Johansen's theory as reported in Table 2.

The load-bearing capacity of the screws connecting the RC slabs to the timber frame has been defined according to the Johansen's equations [CEN 2009, Eq. (8.10)]. The result in Table 3 is obtained by considering a thick steel plate-to-timber connection and a ductile failure mode type e with formation of two plastic hinges, disregarding the contribution from rope effect.

The total characteristic bracing strength, obtained as the sum of the OSB and RC panel contributions, is equal to 34.90 kN. The contribution given by the RC slabs is slightly larger than that given by the OSB panels.

The design of the modular wall panel must also take into account the failure of hold-downs and base shear connections. In a capacity design approach, a suitable overdesign factor should be applied with respect to such failure modes in order to ensure a ductile failure of the bracing system (OSB panel and RC slab) that should result in the weakest part of the structural system. It was assumed that the hold-downs are deputed only to balance the overturning moment on the wall, while the base shear bolts avoid the slip effect (Popovski et al. 2014). According to this simplified approach the maximum base shear forces compatible with hold-down and base shear bolt strengths are 59.9 and 67.9 kN, respectively. These two values are larger than the resistance given by the bracing panels, therefore, the capacity design criteria is ensured.

Experimental Tests

A series of experimental tests was performed to verify the resistance and hysteretic behavior of the investigated construction system. The structural layout and the main characteristics of the

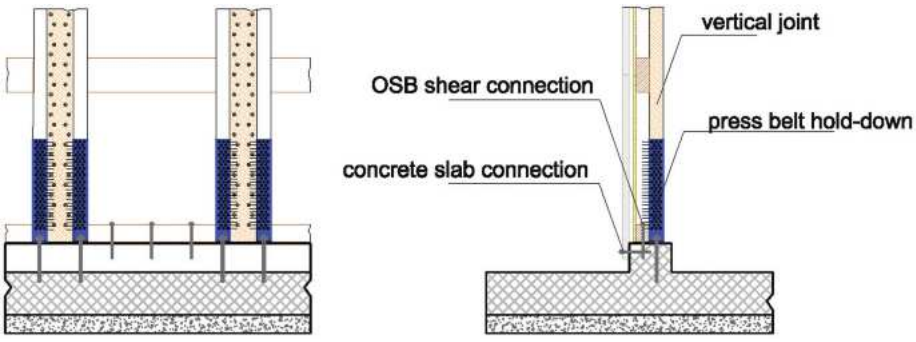

Fig. 4. (Color) Anchoring system of foundations

Table 2. Evaluation of the OSB-Panel Shear Resistance

Geometrical and mechanical parameters	Notations	Values	Units
Equivalent diameter	d_{eq}	1.46	mm
Width of the staple crown	b	12	mm
Spacing of the staples along the edge	i	40	mm
Tensile strength of the wire	f_u	800	MPa
Yielding moment per leg	M_k	886.8	Nmm
OSB-panel thickness	t_{OSB}	15	mm
Load-bearing capacity per staple	F_{k_staple}	0.72	kN
Width of OSB panel	B	820	mm
Characteristic wall panel lateral resistance—OSB contribution	R_{k_OSB}	15.1	kN

Table 3. Evaluation of the RC-Slab Shear Resistance

Geometrical and mechanical parameters	Notations	Values	Units
Screw diameter	d	10	mm
Screw length	L	120	mm
Tensile strength of the screw	f_u	600	MPa
Concrete slab thickness	T_{slab}	40	mm
Timber frame characteristic embedment strength	$f_{h,k}$	25.83	MPa
Characteristic yielding moment	$M_{y,Rk}$	71,659.3	Nmm
Load-bearing capacity per screw	F_{k_screw}	9.90	kN
Number of screws	n.	2	—
Characteristic wall panel lateral resistance—concrete slab contribution	$R_{k,slab}$	19.80	kN

Note: — =.

tested walls (connectors and bracing system) are subsequently described. The test layout, instrumentation, load conditions, and protocol adopted for quasi-static cyclic-loading tests are given. The test results are then reported.

Test Wall Configurations

Three wall configurations were tested: Wall A, aspect ratio 3:1 (3.24 m high, 1.08 m wide—one modular panel); Wall B, aspect ratio 3:2 (3.24 m high, 2.16 m wide—two adjacent modular panels); Wall C, with one opening in the central panel and aspect ratio 1:1 (3.24 m high, 3.24 m long—three adjacent modular panels). For the sake of brevity, only the test results of Walls B and C are presented, being those of Wall A in very good agreement with the others and can be found in (Pozza 2013).

Test Setup and Instrumentation

Walls B and C were tested in separated moments in two different laboratory facilities.

In both cases a RC foundation was realized to reproduce faithfully the base connection in practical applications.

Fig. 5 shows the test setup used for Wall B. An equivalent vertical load of 20 kN/m was applied by three hydraulic actuators placed in correspondence of the vertical wood columns. Lateral guides in contact to the top horizontal beam were used to avoid out-of-plane movement.

Tests on Wall C were carried out on twin walls positioned back-to-back to balance torsional effects and to ensure unidirectional top movement of the specimen. A uniform vertical load of 20 kN/m was applied to the top of each wall by several actuators.

The choice of performing both tests imposing a vertical load of 20 kN/m is coherent with the average gravity load on perimeter walls of a residential three-story building. Moreover, this load condition is aligned with that used to characterize the performance of CLT walls (Ceccotti 2008; Gavric et al. 2011).

Panel and fastener displacements were measured with transducers, placed as shown in Fig. 5.

Test Procedure

Cyclic-loading tests were performed according to EN 12512 (CEN 2006) in displacement control. Such testing protocol requires the preliminary evaluation of the yielding displacement v_y of the specimens. On the basis of the test on the single panel Wall A the reference yielding displacements $v_{y,ref}$ was estimated as 24 mm. Provided that the maximum imposed top displacement cannot exceed the ultimate drift at complete failure of the wall, in practice in both cases it was limited by the test setup. In test on Wall B the maximum elongation of the actuators was 100 mm and testing was stopped before the ultimate strength of the wall could be reached. Also ultimate strength and displacement of Wall C were not reached since the test was stopped at a top displacement of about 80 mm due to the technical limits of the experimental setup in cyclic loading. In any case these displacement limits correspond to interstory drifts of 3.1 and 2.5%, respectively, which are very large if compared with values that shear walls undergo even if subjected to strong seismic events. Furthermore, these limits are aligned with those imposed by various researches on shear-wall seismic performances (e.g., Ceccotti and Sandhaas 2010; Gavric et al. 2014). These limits are sufficient to estimate the seismic capacities of the tested walls. Nevertheless, a monotonic test after the cyclic-loading procedure was carried out on Wall C up to the actual ultimate displacement of the wall.

Test Results

Fig. 6 shows the results which plots the imposed top displacement and the corresponding force applied by the actuator. The load-slip curve of Wall B is asymmetric because only pull cycles could be carried out at the maximum amplitude, since the lateral guides demonstrated to be insufficient to prevent the out-of-plane instability of the wall under high push forces.

During the cyclic phase, Wall C did not exhibit failure or substantial strength-degrading phenomena, as Fig. 6 shows. To verify the ultimate lateral load resistance and ductility of the system, a ramp monotonic test up to collapse was performed on Wall C according to EN 594 (CEN 2011), after the completion of the cyclic test. The softening branch started after a top displacement of 220 mm (drift 6.79%).

Walls B and C show the typical hysteretic behavior of steel-wood and wood-wood connections characterized by pinching. The tested walls also showed marked hardening due to the large-diameter connectors used to fix the concrete slabs to the wood frame.

Fig. 7 shows the two tested walls at the end of the cyclic tests. No damages are evident, except for a permanent dislocation of the concrete slabs.

Fig. 8 shows that Wall C exhibited significant shear deformation of the bracing system at the end of the test, with substantial relative sliding between slabs. Despite the strong shear deformation of the wall, the slabs did not show any brittle failure or large cracks near the fastening points. This experimental evidence shows that the connection system used to fix the slabs to the frame was designed to ensure ductile failure of the bracing system, with the formation of plastic hinges in the screws near the wood-concrete interface

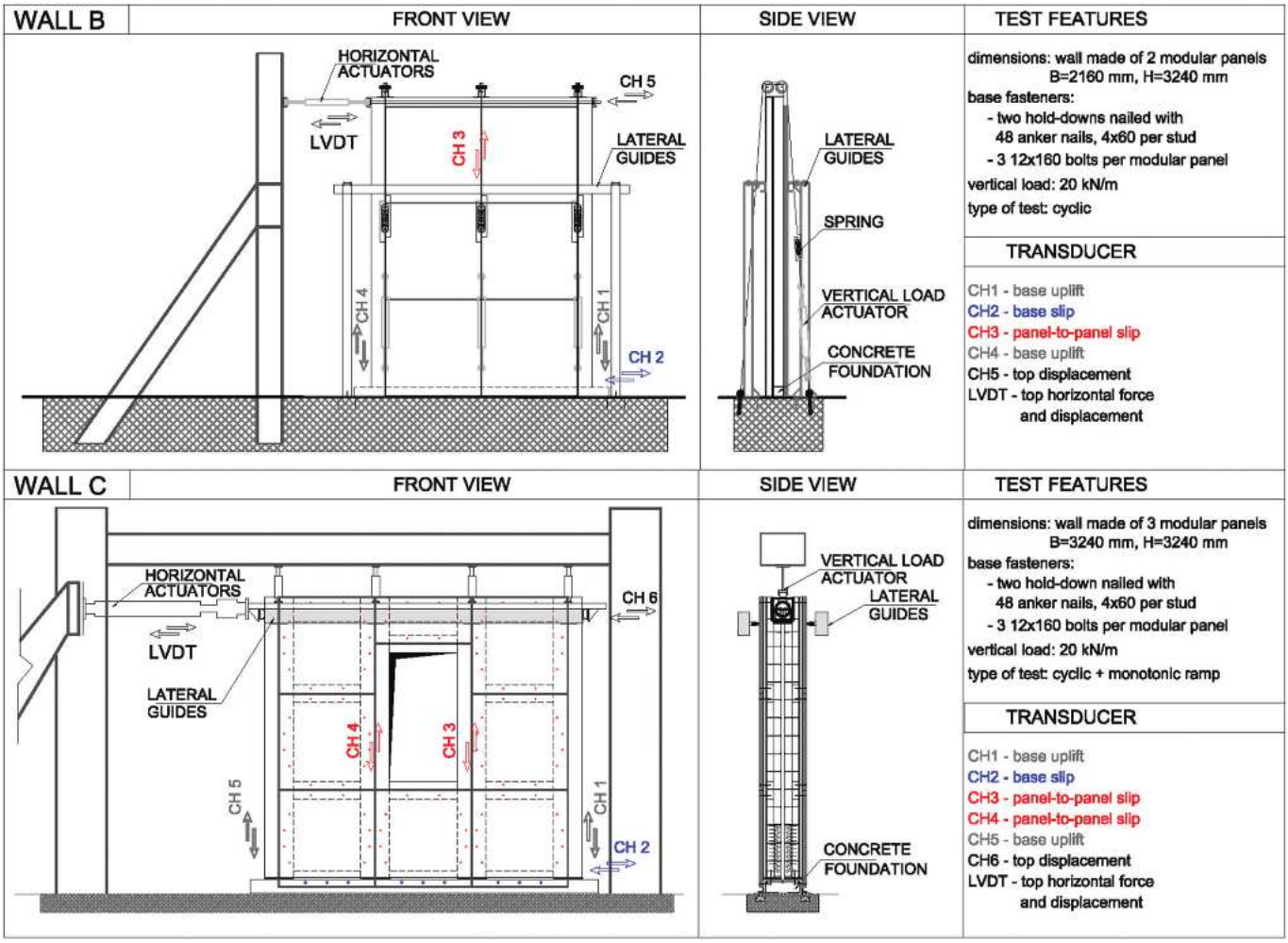

Fig. 5. (Color) Experimental setup for Walls B and C

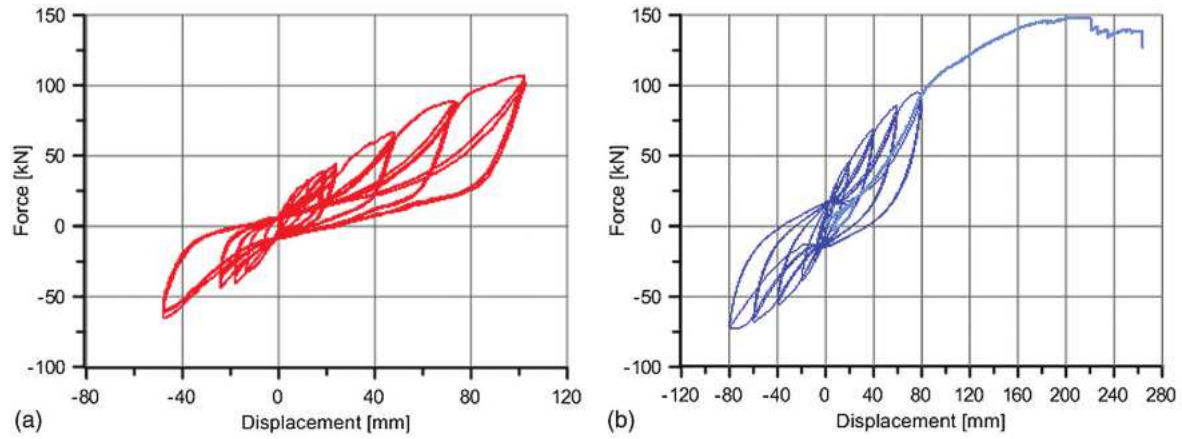

Fig. 6. (Color) Load displacement curve of cyclic-loading tests: (a) Wall B; (b) Wall C

(Fig. 8). Deformation of the base fasteners during cyclic testing was modest, and only at the end of monotonic tests some failures occurred in the base hold-down, due to excessive wall uplift (Fig. 8). Fig. 9 shows results of tests on connections. Fig. 9 also shows that the deformation of the system was mainly due to the shear deformation of the bracing system, whereas the connections showed modest displacements thanks to the overdesign factor applied. Such experimental evidence is consistent with the adopted capacity-design criteria.

Analysis of Experimental Results

The cyclic test results were analyzed to define the structural properties of this newly developed shear-wall system. This section reports

J. Struct. Eng.

(a) (b)

Fig. 7. (Color) Wall configuration at end of cyclic testing: (a) Wall B; (b) Wall C

(a) (b) (c) (d)

Fig. 8. (Color) Wall C configuration at end of monotonic ramp test and details of failure: (a) shear wall at maximum applied displacement; (b) concrete slab after test; (c) base hold-down; (d) screw

and critically discusses the evaluation of the following mechanical characteristics: yielding limit, ultimate conditions, stiffness for the elastic and hardening branches, maximum ductility achieved during testing, and strength degradation at each level of ductility. A comparison with the design provisions is shown with regard to seismic (ductility class) characteristics.

Ductility Estimation

Ductility is an important requirement in seismic design. An extensive discussion about the procedures that can be used for ductility estimation can be found in Muñoz et al. (2008). In this work the method based on EN 12512 provisions (CEN 2006) was used to define the ductility ratio of the investigated shear walls. The envelope curves which best fit the cyclic experimental hysteresis load-slip curves were defined according to the three-parameter formulation of Foschi and Bonac (1977). Since the final failure condition was not actually achieved for Wall B, the maximum displacement and force reached during the last test cycle were conventionally assumed as the failure limit. For Wall C, the failure displacement was assumed as that corresponding to the maximum force achieved during monotonic ramp testing.

A conventional ultimate displacement equal to 80 mm has been adopted in several seismic characterization tests of timber shear walls (Ceccotti 2008). To allow a comparison between the proposed hybrid system with other systems (e.g., CLT), the ductility ratios were also evaluated assuming as ultimate top displacement the conventional value 80 mm. Table 4 lists the failure forces, displacement values, and ductility for both the tested walls and for both the effective and conventional ultimate displacements.

The experimental load-displacement curves of the tested walls show a well-defined hardening phase, whereas the elastic branch is nonlinear, with continuous stiffness modification. Due to these peculiarities, some limitations to the applicability of bilinearization criteria exist. In fact, method (b) of EN 12512 (CEN 2006) assumes that the value of hardening stiffness be 1/6 of the initial elastic stiffness, without taking into account the actual hardening stiffness. Due to the specific shape of the experimental load-slip curve, the tangency condition between the hardening branch and the envelope curve cannot be obtained and, consequently, hence the EN-b approach cannot be applied. Therefore the yielding condition was defined only with reference to the EN-a approach. Table 4 lists the main results in terms of elastic and hardening stiffness, strength, displacements, and ductility ratios.

Notice that the yielding displacement obtained with the EN-a approach is about 10 mm for both the walls, lower than that initially estimated on the basis of the test on a single panel (test A). This unexpected initial stiffness of the walls has been ascribed to the redundancy of the ground connections in multipanel walls. The lower values of the yielding displacement result in high-ductility

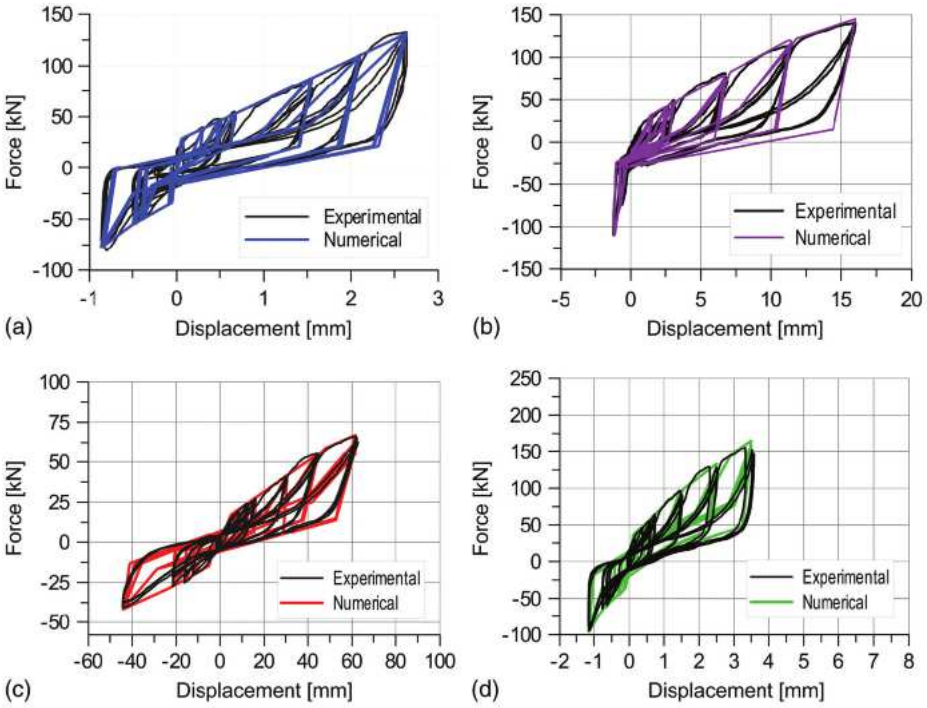

Fig. 9. (Color) Results on connections for Wall B: (a) angle bracket; (b) hold-down; (c) bracing system; (d) vertical joint

Table 4. Test Results and Interpretation according to EN 12512 Approach (Data from CEN 2006)

Parameters		Wall B	Wall C
Ultimate displacement	V_u (mm)	102.0	182.1
Ultimate force	F_u (kN)	112.6	145.7
Elastic stiffness	α(kN/mm)	4.4	4.6
Hardening stiffness	β(kN/mm)	1.1	1.1
Yielding displacement	V_y (mm)	10.3	10.2
Yielding force	F_y (kN)	41.4	54.9
Ductility ratio_V_u	$\mu = V_u/V_y$	9.9	17.4
Ductility ratio_ 80 mm	$\mu = 80/V_y$	7.8	7.8

values, always larger than six, which is the minimum value to be assured by HDC shear walls. The ductility value of Wall B is lower than that of Wall C, but this difference is clearly due to the conservative assumption of the failure condition of the former. Comparing the ductility values obtained with the conventional ultimate displacement limit of 80 mm with other studies (Gavric et al. 2011; Pozza et al. 2014), the ductility of this novel system is always greater than that obtained for massive timber systems (e.g., CLT). This is because the shear deformation of the bracing panels allows the achievement of higher ductility than shear walls in which the dissipative capacity is mainly concentrated in the connection system.

Strength Degradation and Viscous Damping Ratio

Wooden structures assembled using metal fasteners are sensitive to stiffness and strength degradation of connection elements when undergoing cyclic action. The consequent strength impairment is an important parameter in identifying the ability of a wooden structure to resist cyclic action and, therefore, seismic shocks. According to Eurocode 8 (CEN 2013), this parameter and the ductility ratio are used to define the ductility class of a timber structure. Table 5 lists the strength degradation recorded between the first and third cycles of each displacement level of the test walls.

Table 5. Strength Degradations at Each Cycle Amplitude

Cycle amplitude (mm)	Strength reduction (%)	ν_{eq} (%)
	Wall B	
12	3.5	14.52
24	4.7	13.90
48	6.7	12.61
72	6.9	9.04
102	7.1	7.68
	Wall C	
10	2.5	14.74
20	5.9	13.60
40	7.8	13.27
60	8.5	12.9
80	9.5	11.7

Table 5 shows that the loss in strength increases with cycle amplitude, but is always lower than 10% for both walls. These values confirm the good behavior of the system under cyclic action and, therefore, its suitability for use in seismic areas.

Another parameter adopted to summarize the hysteretic properties of a structural system is the equivalent viscous damping ν_{eq}. According to EN 12512 (CEN 2006), it is defined with reference to the third cycle of each ductility level. Table 5 shows these results. Note that ν_{eq} is always greater than 7%, confirming a sufficient dissipative capability of this system.

A comparison with other timber construction systems can be done also in terms of ν_{eq}. Comparing the values in Table 5 with those reported in Pozza et al. (2014) for massive timber shear walls, it can be stressed that at low-level drifts the hybrid system presents higher values than common CLT systems, being aligned with

platform-frame system. For higher drifts this value decreases due to pinching phenomenon, analogously to other timber structural systems.

Comparisons with Seismic Design Provisions

Eurocode 8 (CEN 2013) provides three ductility classes (low, medium, high) depending on the dissipative capacity of timber constructive system. The parameters used to classify timber structures into the correct ductility class are the ductility ratio and the strength degrading value. A ductility ratio of 4 is required for the medium ductility class and 6 for the high ductility class. In both cases, strength impairment must be lower than 20%.

Both the tested walls presented ductility ratios greater than 6—both for the actual and the conventional ultimate displacement capacity. Strength degradation was also always lower than 20%. According to the Eurocode 8 (CEN 2013), the investigated hybrid construction system fulfills the requirements to be assigned to the high ductility class (HDC).

This classification certifies the good dissipative capacity of the studied wooden shear wall, but does not define exactly the most suitable q-factor for seismic design. The proposed construction system does not fit exactly with the standard building typologies listed in Eurocode 8 (CEN 2013, Table 8.1). It may be treated as platform-frame technology, for which the q-factor for the HDC ranges between 3 and 5 (CEN 2013). According to Ceccotti and Sandhaas (2010), numerical simulations with nonlinear finite-element models able to reproduce the hysteretic behavior of the hybrid shear walls have been used to derive the proper q-factor for the proposed construction system.

Numerical Modeling of Experimental Tests

The numerical procedure for q-factor evaluation (Ceccotti and Sandhaas 2010) is based on experimental results from simple elements as input data in numerical modeling of complex buildings, for which nonlinear dynamic (NLD) analyses can be performed. In the numerical model, the hysteretic response of each connector used to assemble the shear wall is introduced and calibrated against experimental results.

The numerical model of shear wall uses the hypothesis that nonlinear wall behavior is concentrated in the connectors and bracing systems, whereas the wood frame remains elastic. Basic elementary components have been used: linear truss for timber frame, equivalent inelastic link for the bracing system (stapled OSB panel plus screwed RC slab), inelastic springs for hold-downs, base shear bolts and in-plane vertical joints between adjacent wall modules. The inelastic link representing the bracing system considers together the cumulated response of OSB panels and RC slabs. The research-oriented numerical code "Open System for Earthquake Engineering Simulation—OPENSEES" (Fenves 2005) and the hysteresis model developed by K. Elwood (Elwood and Moehle 2006) were used to simulate the behavior of each component (Fig. 9). All inelastic components follow pinched load-displacement curves with degradation under repeated cyclic loading in order to reproduce faithfully the actual hysteretic response of walls.

After calibration of the elementary nonlinear connections, the cyclic tests on Walls B and C were simulated, by imposing a horizontal top displacement and a constant vertical load to the top of the wall. Fig. 10 shows the scheme of the numerical models used for the analysis.

The load-displacement curves of Fig. 11 show the good match between experimental results and numerical simulations. The good quality of the model was further confirmed by assessment of dissipated energy per cycle between the experimental tests and the numerical simulations shown in Fig. 11: the maximum difference is 11.5% for Wall B and 8.5% for Wall C (values referring to maximum amplitude cycle in traction).

Assessment of Behavior q-Factor of a Case Study Building

The force-based design method (FMD) (Chopra 1995) is an engineering approach for seismic building design and refers to inertial forces induced in structures by seismic action. Its application requires evaluation of the most suitable q-factor, which summarizes the postelastic behavior and ductility of the building. In this work, the q-factor defined by the PGA approach was considered appropriate (Ceccotti and Sandhaas 2010). This method disregards the actual yielding limit of structures and the q-factor is defined as the ratio between the acceleration which brings the structure to the *near-collapse condition* (i.e., PGA_{u_eff}) and that used for the elastic design of the building (PGA_{u_code}). Ceccotti and Sandhaas (2010) reported the PGA-based method that consists of the following steps:

1. Choice of a case-study building and design according to the relevant static and seismic code, assuming $q = 1$, so that the building can elastically resist the PGA_{u_code} value;
2. Modeling the test buildings with finite-element models capable of reproducing the hysteretic behavior of the connection elements and calibrated against experimental results;

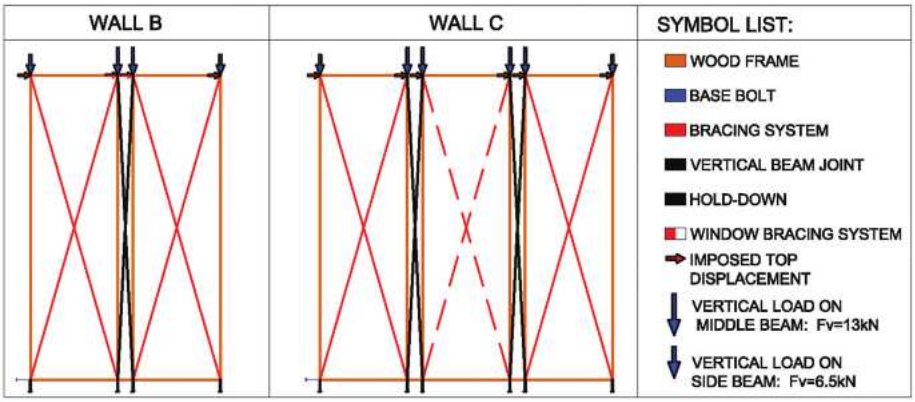

Fig. 10. (Color) FEM model: Wall B and Wall C

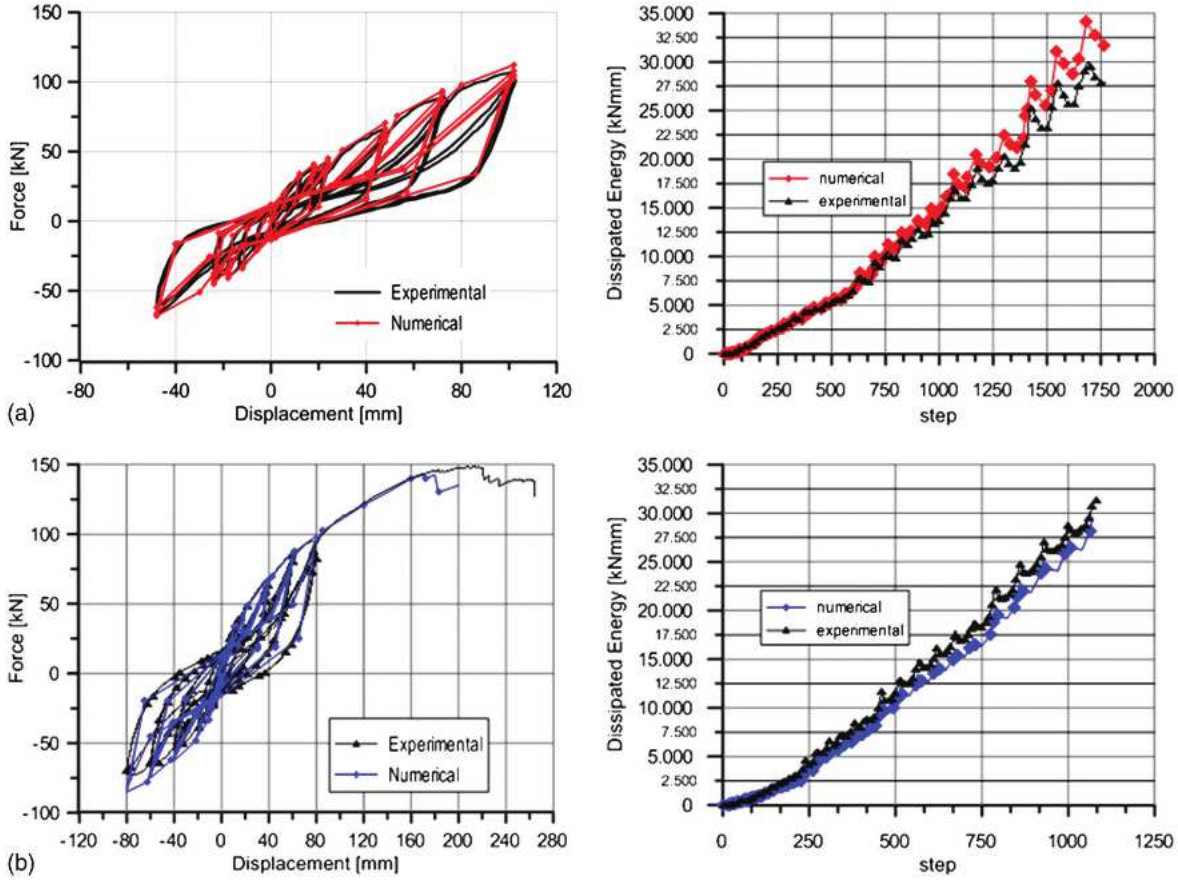

Fig. 11. (Color) Comparisons between experimental results and FEM simulation in terms of load-slip curves and dissipated energy: (a) Wall B; (b) Wall C

3. Definition of an ultimate or near-collapse condition of the building, which coincides with the ultimate displacement of fastening elements;
4. Assessment of the seismic intensity (PGA_{u_eff}) which leads to the ultimate condition through a series of NLD analyses, with gradual increments of PGA intensity; and
5. Determination of the most suitable q-factor according to the PGA-based approach.

The main hypothesis of this method is that a building reaches its yielding condition when $PGA_{\_design}$ is reached and is constant, independent of seismic frequency content. In addition, this q-factor definition is code-dependent, because it represents a conventional value based on seismic building design according to a specific seismic code. Such a definition already includes the overstrength corrective factor, defined as the ratio between the actual yielding strength and the design strength of the structure (Elnashai and Mwafy 2002).

Case-Study Building

In order to define the actual seismic performance of the plated shear-wall system and to make direct comparisons with cross laminated timber, the same three-story CLT building tested on the shaking table during the SOFIE project was examined (Ceccotti 2008). Configuration B with symmetric openings on the ground floor was chosen. Fig. 12 shows that the geometrical layout of this building was compatible with the precast modular dimension of the system.

Thanks to the inplan symmetrical distribution of the shear walls, the case study building could be studied with two independent 2D plane models along both directions. In this work, analyses focused on the wall placed along direction X, which has one door opening 2-m wide on the ground floor. Two mass configurations were studied in order to verify the influence of the principal period of vibration on the seismic response of the building. The difference between the two case studies in terms of total mass was about 25%. Table 6 lists the story mass distribution and principal elastic period T_1 of each building.

Seismic Design of Case Study Buildings

It was assumed that the case study buildings were assembled with the same modular panels subjected to the cyclic tests described in the previous sections. The seismic design of the buildings was based on the lateral shear resistance of the single precast modular panel and on evaluation of the maximum PGA_{u_code} compatible with base shear resistance by linear static analysis, comprising the following data (CEN 2013): type 1 elastic response spectra and rock foundation (type A soil, corresponding to $S = 1.0$, $T_B = 0.15$ s, $T_C = 0.4$ s, $T_D = 2.0$ s); behavior factor $q = 1$; and lowest bound factor for design spectrum $\beta = 0.20$.

Evaluation of q-Factor

Fig. 13 shows the numerical model of the wall with type and position of nonlinear springs and story masses.

Several NLD analyses were performed to evaluate the most suitable q-factor for this system and seven artificially generated seismic shocks were simulated in order to meet spectrum compatibility

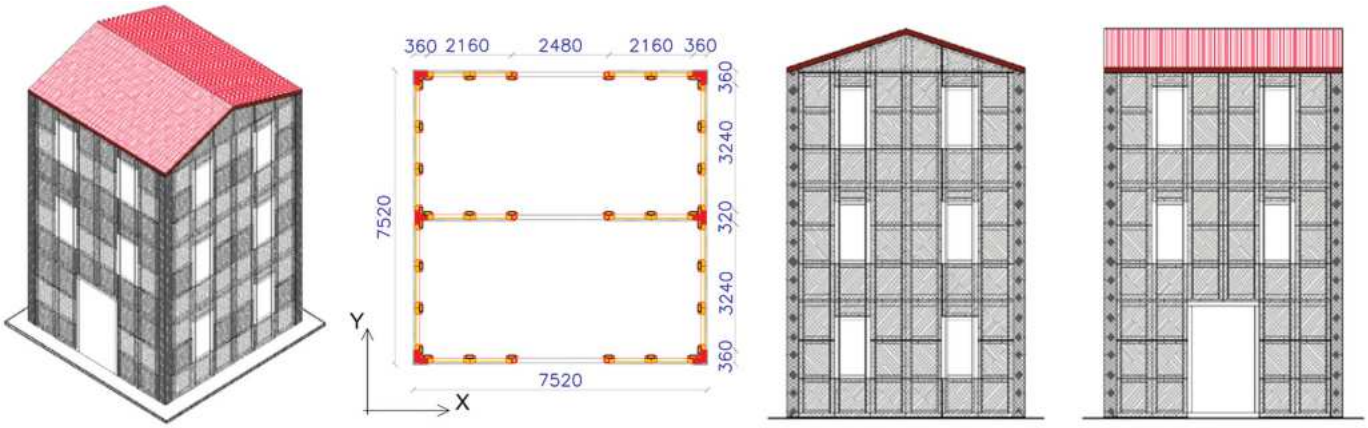

Fig. 12. (Color) Case study: modular wall panel arrangement

Table 6. Mass Distributions Analyzed

Building	1st story (t)	2nd story (t)	3rd story (t)	Total (t)	T_1 (s)
N.1	16.5	16.5	12.7	45.7	0.48
N.2	10.7	10.7	8.4	29.8	0.32

requirements. Dynamic equilibrium equations were integrated with time steps of 0.001 s, with equivalent viscous damping of 2%, according to the Rayleigh model. The choice of the damping coefficient was made according to Ceccotti and Sandhaas (2010). Both test buildings were subjected to increasing levels of seismic intensity, from the peak acceleration value of PGA_{u_code} to the near-collapse condition (PGA_{u_eff}), which was stated as the first time the ultimate displacement of the bracing system or base joints was reached. The near-collapse condition was defined with the criteria reported by Pozza (2013). In detail, the effective failure condition of the connection elements was used as a reference—for the hold-downs, this condition corresponded to an uplift of 25 mm; and for the shear connections (i.e., base bolts, vertical panel-to-panel joints, and bracing system), the failure condition corresponded to interstory drift of 2.5%. Table 7 lists the PGA_{u_eff} bringing the buildings to the near-collapse condition and the relative q-factor values (Fig. 14).

Although the yielding limit of the structure had been fixed, the obtained q-factor values showed moderate variability, between 3.9 and 4.6. This means that the effect of the frequency content of the seismic signals is not important to define the failure condition.

According to the analyses, the q-factors converge on a value of 4, confirming the good dissipative capability of this construction system, as this value falls within the range of the high ductility class (CEN 2013).

It must be stressed that the obtained results cannot be used to derive general conclusions about the correct q-factor to be used in designing plated shear-wall systems such as this one, since they are based on the analysis of a single three-story case study building. For more accurate and reliable evaluation of q-factor variability with building characteristics (i.e., number of stories, arrangement

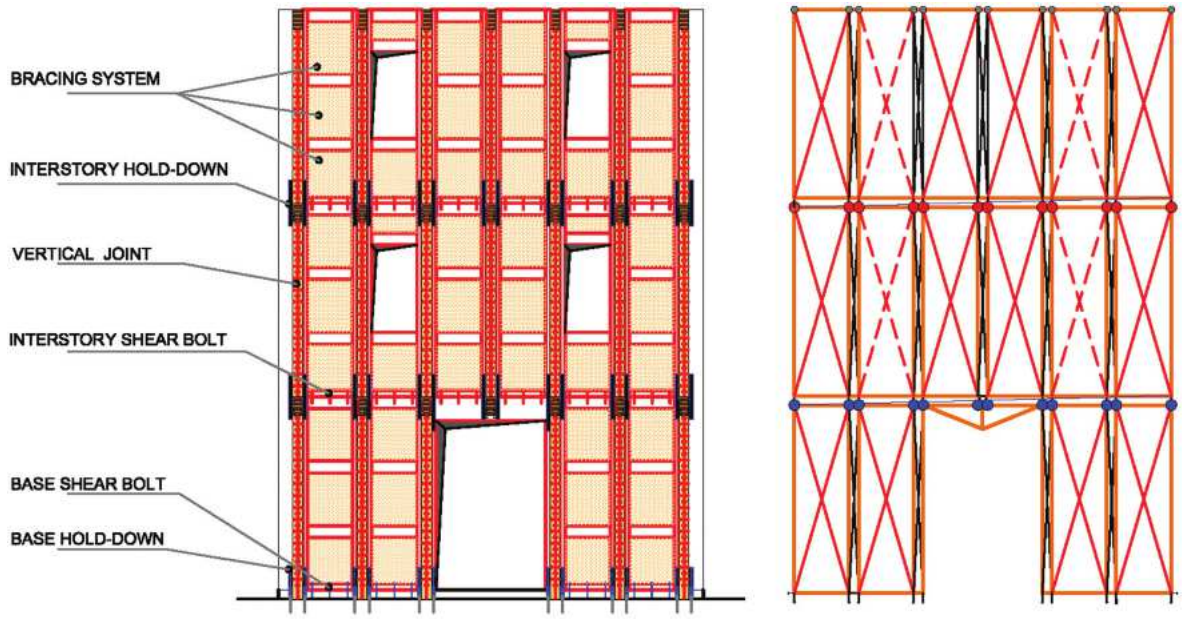

Fig. 13. (Color) Wall panels: arrangement of fasteners and bracing system, FEM model, position of nonlinear elements, and mass

Table 7. PGA_{u_eff} Values and q-Factor for Seismic Shocks Tested for Both Study Buildings

	Building test 1		Building test 2	
Seismic signals	PGA_{u_eff}	q	PGA_{u_eff}	q
Earthquake 1	0.82	4.6	1.05	4.4
Earthquake 2	0.77	4.3	0.91	3.8
Earthquake 3	0.72	4.0	0.97	4.0
Earthquake 4	0.78	4.3	1.02	4.3
Earthquake 5	0.70	3.9	1.07	4.5
Earthquake 6	0.75	4.2	0.96	4.0
Earthquake 7	0.73	4.1	0.99	4.1
Average	0.75	4.2	1.00	4.1
Minimum	0.70	3.9	0.91	3.8
Maximum	0.82	4.6	1.07	4.5

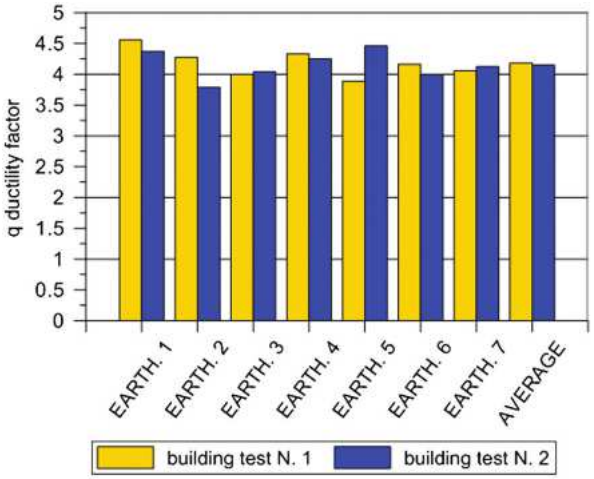

Fig. 14. (Color) q-factor for the considered earthquakes and for both the examined buildings

of resistant plated shear walls), more case studies must be numerically investigated. Three-dimensional numerical models must also be used to explain the effects of plan irregularities and those of the T or L corners between shear walls.

Conclusions

The newly developed wood-concrete system represents a viable alternative to the more traditional and common timber building technologies, such as classical platform-frame systems and the massive CLT system. The major innovation of this work is that the outer RC skin improves strength and ductility against horizontal loads (i.e., seismic shocks).

Original and trustable information about the seismic behavior of the investigated construction system is reported in the paper. It is interpreted by means of a well-assessed and accepted analytical and numerical methodology.

The experimental results show that the investigated hybrid shear walls have limited strength degradation, good dissipative capacity, and high ductility. All properties, which make the construction technology suitable for use in seismic areas and classifiable as HDC.

The seismic design of this system can be performed with the well-known FMD method (Chopra 1995), considering a q-factor up to 4, as demonstrated by the experimental and numerical analyses reported in this work.

Acknowledgments

The research has been supported by Polifar s.r.l. The authors gratefully acknowledge the kind collaboration of the staff at the Mechanical Testing Laboratory of the CNR—IVALSA, San Michele all'Adige TN—Italy.

References

Amadio, C., Gattesco, N., and Urban, F. (2007). "Experimental study of timber shear walls made with OSB or wood fiber-reinforced gypsum panels." *Proc., ANIDS*, Univ. of Pisa, Pisa, Italy.

Ceccotti, A. (2008). "New technologies for construction of medium-rise buildings in seismic regions: The XLAM case." *Struct. Eng. Int.*, 18(2), 156–165.

Ceccotti, A., and Sandhaas, C. (2010). "A proposal for a standard procedure to establish the seismic behaviour factor q of timber buildings." *Proc., 11th World Conf. on Timber Engineering WCTE*, Trees and Timber Institute, National Research Council, San Michele all'Adige, TN, Italy.

CEN European Committee for Standardization. (2006). "Timber structures—Test methods—Cyclic testing of joints made with mechanical fasteners." *EN 12512*, CEN, Brussels, Belgium.

CEN European Committee for Standardization. (2009). "Design of timber structures—Part 1-1: General—Common rules and rules for buildings." *Eurocode 5*, CEN, Brussels, Belgium.

CEN European Committee for Standardization. (2011). "Timber structures—Test methods—Racking strength and stiffness of timber frame wall panels." *EN 594*, CEN, Brussels, Belgium.

CEN European Committee for Standardization. (2013). "Design of structures for earthquake resistance—Part 1: General rules, seismic actions and rules for buildings." *Eurocode 8*, CEN, Brussels, Belgium.

Chopra, A. K. (1995). *Dynamics of structures—Theory and applications to earthquake engineering*, Prentice Hall, Upper Saddle River, NJ.

Elnashai, A. S., and Mwafy, A. M. (2002). "Overstrength and force reduction factors of multistorey reinforced-concrete buildings." *Struct. Des. Tall Build.*, 11(5), 329–351.

Elwood, K. J., and Moehle, J. P. (2006). "Idealized backbone model for existing reinforced concrete columns and comparisons with FEMA 356 criteria." *Struct. Des. Tall Spec. Build.*, 15(5), 553–569.

Fenves, G. L. (2005). *Annual workshop on open system for earthquake engineering simulation*, Univ. of California, Berkeley, CA.

Foschi, R. O., and Bonac, T. (1977). "Load slip characteristic for connections with common nails." *Wood. Sci.*, 9(3), 118–123.

Gavric, I., Ceccotti, A., and Fragiacomo, M. (2011). "Experimental cyclic tests on cross-laminated timber panels and typical connections." *Proc., ANIDIS*, Politecnico di Bari, Bari, Italy.

Gavric, I., Fragiacomo, M., Popovski, M., and Ceccotti, A. (2014). "Behaviour of cross-laminated timber panels under cyclic loads." *Materials and Joints in Timber Structures*, Vol. 9, Springer, Netherlands, 689–702.

Karacabeyli, E., and Ceccotti, A. (1997). "Seismic force modification factor for design of multi-storey wood-frame platform construction." *Proc., Meeting 30 of the Working Commission W18-Timber Structures, Paper CIB-W18/30-15-3*, CIB, Vancouver, Canada.

Muñoz, W., Mohammad, M., Salenikovich, A., and Quenneville, P. (2008). "Need for a harmonized approach for calculations of ductility of timber assemblies." *Proc., Meeting 41 of the Working Commission W18-Timber Structures, Paper CIB-W18/41-15-1*, CIB, St. Andrews, Canada.

Popovski, M., Pei, S., van de Lindt, J. W., and Karacabeyli, E. (2014). "Force modification factors for CLT structures for NBCC."

Materials and joints in timber structures, Vol. 9, Springer, Netherlands, 543–553.

Pozza, L. (2013). "Ductility and behaviour factor of wood structural systems—Theoretical and experimental development of a high ductility wood-concrete shearwall system." Ph.D. dissertation, Dept. of Civil Architectural and Environmental Engineering, Univ. of Padova, Padova, Italy.

Pozza, L., Scotta, R., Trutalli, D., Pinna, M., Polastri, A., and Bertoni, P. (2014). "Experimental and numerical analyses of new massive wooden shear-wall systems." *Buildings*, 4(3), 355–374.

Vahik, E. (2006). "TF2000 timber-frame building was tested at BRE Cardington. Barrier to the enhanced use of wood in construction." *Time for Timber in Europe Conf.*, BRE Centre for Timber Technology and Construction, Cardington, Bedfordshire, U.K.